RSC Advances

PAPER

View Article Online
View Journal | View Issue

Cite this: *RSC Adv.*, 2023, **13**, 20351

Fe_3O_4@ABA-aniline-CuI nanocomposite as a highly efficient and reusable nanocatalyst for the synthesis of benzothiazole-sulfide aryls and heteroaryls†

Mingzhe Sun,*[a] Wei Liu,[b] Wei Wu,[b] Qun Li[a] and Li Shen *[c]

Studying diaryl sulfides and benzothiazoles is important in organic synthesis because numerous natural and medicinal products contain these scaffolds. Over the past few years, research on the synthesis of compounds containing benzothiazole-sulfide aryls, as important biological molecules, has received significant attention. Multicomponent reactions are the most popular strategy for performing difficult reactions and the synthesis of complexed molecules such as benzothiazole-sulfide aryls. In this work, CuI was successfully immobilized on the surface of magnetic Fe_3O_4 nanoparticles modified with aniline and 4-aminobenzoic acid [Fe_3O_4@ABA-Aniline-CuI nanocomposite] and its catalytic activity was investigated in the preparation of a broad range of benzothiazole-sulfide aryls and heteroaryls through the one-pot three-component reactions of 2-iodoaniline with carbon disulfide and aryl or heteroaryl iodides in the presence of KOAc as base in PEG-400 as solvent. TEM and SEM images revealed that the shape of the Fe_3O_4@ABA-Aniline-CuI particles is spherical and the size of the particles is approximately between 12–25 nanometers.

Received 8th May 2023
Accepted 21st June 2023

DOI: 10.1039/d3ra03069e

rsc.li/rsc-advances

Introduction

Catalysts are the most important materials in chemical processes, and during the last decade, research on them has become one of the most important topics among chemists.[1–5] In the new era of chemistry, especially organic chemistry, chemists are always looking for environmentally friendly, cost-effective and efficient catalytic systems to perform chemical processes.[6–11] Each type of catalyst has advantages and disadvantages.[12–14] Two characteristics of efficient catalysts are their high activity and high selectivity.[7] One of the most important goals of modern chemistry is to combine the benefits of both heterogeneous and homogeneous catalysts.[15–19] Nanocatalysts have the advantages of both the mentioned systems and their activity, selectivity, high stability and ability to be recovered from the reaction medium.[20–22] Nanoparticles are a group of materials that are artificially produced by combining atoms, molecules or groups of them.[23–25] Magnetic nanoparticles are particles smaller than one hundred nanometers that have magnetic properties in the presence of an external magnetic field.[26,27] Clumping is one of the disadvantages of magnetic nanoparticles as catalysts and functionalizing the surface of magnetic nanoparticles is a suitable way to solve this problem.[28–30] Fe_3O_4 nanoparticles are well known and can be used as a suitable support for functionalization with metals, organic catalysts, N-heterocyclic carbenes and chiral catalysts.[31–33] Recent advances have shown that the improvement of catalyst performance can be achieved through structural modifications of magnetic nanoparticles.[34] Using Fe_3O_4 NPs as a support substrate, modern catalysts that have higher specific surface area than conventional catalysts can be obtained, and in addition to consuming fewer precious metals, their efficiency, which makes creating a catalyst cheaper and more effective, can be increased.[35–37] Magnetic nanocatalysts are easily synthesized and can be reused several times without losing a significant amount of their activity by being recycled through an external magnetic field.[38]

The chemistry of heterocyclic compounds, which deals with the properties, synthesis, and applications of this class of compounds, is considered an important branch of organic chemistry.[39,40] On the other hand, research on organosulfur chemistry (compounds containing S element) is one of the most important topics in medicinal, pharmaceutical and industrial chemistry.[41,42] Benzothiazoles are a class of aberrant compounds that have a benzene ring fused to a thiazole ring.[43,44] A useful central structure, benzothiazole forms part of the molecular structure of a large number of biological molecules,

[a]College of Food and Biology, Changchun Polytechnic, Changchun, Jilin 130033, China. E-mail: mingzhesun2021@163.com
[b]College of computer science, Jilin Normal University, Siping, Jilin 136000, China
[c]Institute Chemical and Nanotechnology, Beijing, China. E-mail: lshenl1985@gmail.com

† Electronic supplementary information (ESI) available. See DOI: https://doi.org/10.1039/d3ra03069e

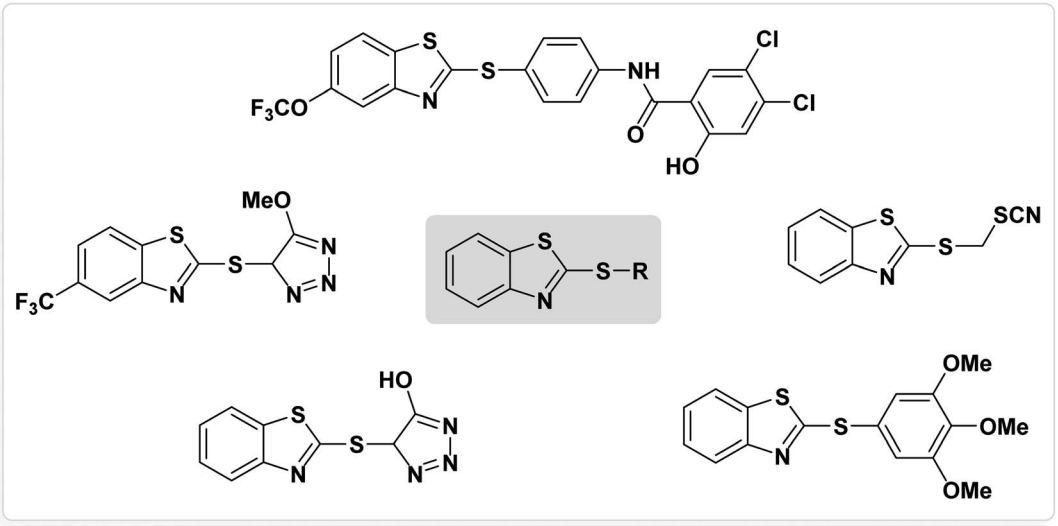

Fig. 1 Several bioactive molecules containing benzothiazole-sulfide scaffolds.

drugs, natural products and industrial chemicals.[45–47] Recently, applications of benzothiazoles with different biological activities, such as anti-viral, anti-tumor, anti-fungal, anti-bacterial and anti-cancer activities, have been discovered.[43,46] In the past few decades, the formation of carbon-sulfur bonds has been widely studied by chemists. Studying diaryl sulfides is

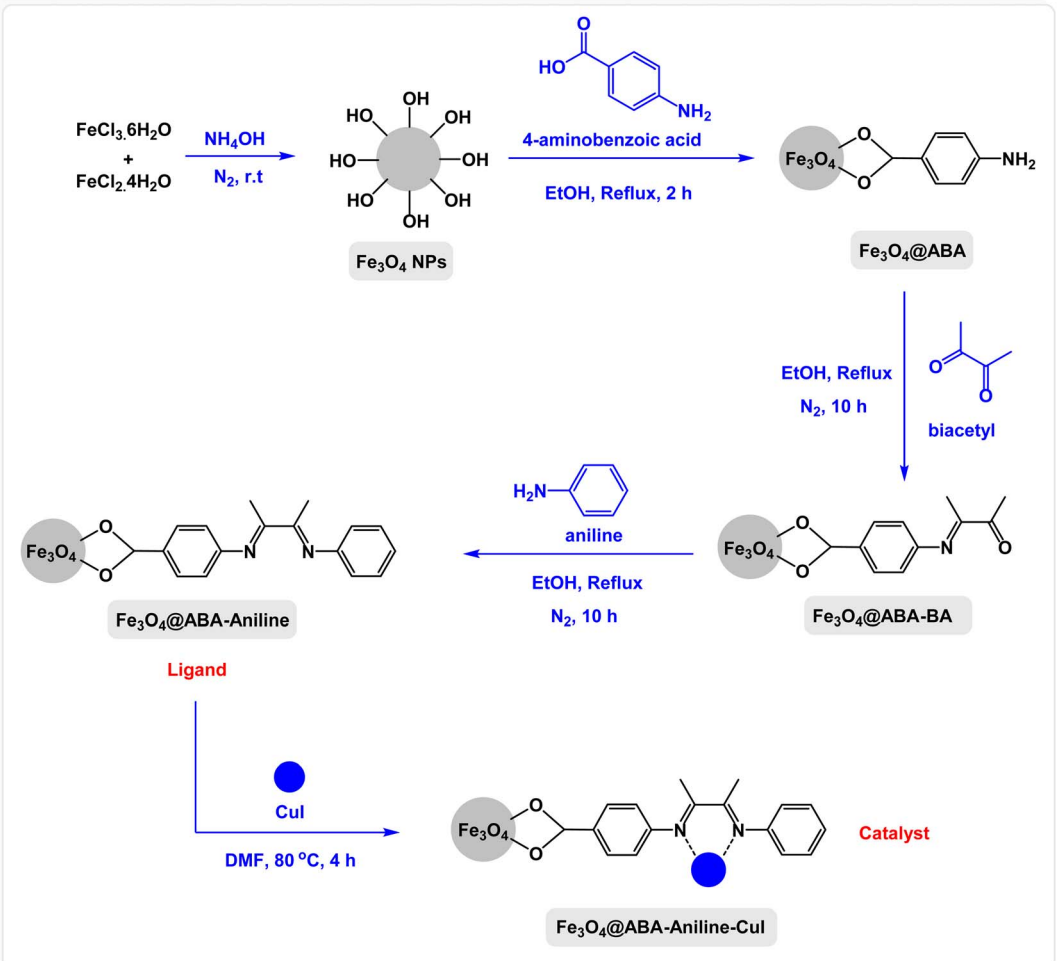

Scheme 1 Steps of fabrication of Fe_3O_4@ABA-Aniline-CuI nanocatalyst.

important in organic synthesis because a large number of natural and medicinal products contain sulfide scaffolds.[48–50] Diaryl sulfides are one of the most important sulfur-containing organic compounds in the chemical, biochemical, biological and industrial industries.[51–53] Therefore, extensive studies have been conducted in order to provide new methods for the synthesis of these compounds. Compounds containing benzothiazole-sulfide aryls are unique, important heterocyclic and organosulfur compounds with many biological and pharmacological activities.[54] Several bioactive molecules containing benzothiazole-sulfide scaffolds are listed in Fig. 1.[54–56]

Therefore, the development of an effective methodology for the synthesis of benzothiazole-sulfide aryls is an important research challenge with high potential for beneficial applications in the pharmaceutical industry. Multicomponent reactions are the most popular strategy for difficult reactions and the synthesis of complexed molecules such as benzothiazole-sulfide aryls. In order to explore the potential of benzothiazole-sulfide aryl compounds, we developed an efficient protocol to synthesize various analogues of benzothiazole-sulfide aryl compounds from 2-haloaniline, aryl halides and carbon disulfide as the sulfur source for both the benzothiazole and sulfide moieties. A typical reaction was carried out over heterogeneous Cu complex as catalyst and the target compounds were obtained in excellent yields.

Result and discussion

In this paper, we report the fabrication of Fe_3O_4@ABA-Aniline-CuI nanocomposite as a novel and efficient magnetic catalyst for the synthesis of a broad range of benzothiazole-sulfide aryls and heteroaryls through the one-pot three-component reactions of 2-iodoaniline with carbon disulfide and aryl or heteroaryl iodides in the presence of KOAc as base in PEG-400 as solvent. The steps of the fabrication of Fe_3O_4@ABA-Aniline-CuI nanocomposite are outlined in Scheme 1. First, magnetic iron nanoparticles were synthesized from Fe(II) and Fe(III) salts utilizing the coprecipitation procedure, then these nanoparticles were coated with 4-aminobenzoic acid. A suitable ligand (Fe_3O_4@ABA-Aniline nanocomposite) was prepared from the reaction of Fe_3O_4@ABA-BA (prepared from the treatment of Fe_3O_4@ABA with biacetyl) with aniline in ethanol solvent under reflux conditions. In the last step, by fixing copper iodide on the surface of Fe_3O_4@ABA-Aniline nanoparticles, the final catalyst [Fe_3O_4@ABA-Aniline-CuI] was successfully synthesized.

Characterization of Fe_3O_4@ABA-Aniline-CuI nanocatalyst

After designing and fabricating the nanocatalyst (Fe_3O_4@ABA-Aniline-CuI), various techniques were used to identify the catalyst.

FR-IR spectroscopy

By using FT-IR spectroscopy and comparing the spectra of Fe_3O_4@ABA-Aniline ligand and Fe_3O_4@ABA-Aniline-CuI (Fig. 2), it is possible to understand the successful functionalization of the functional groups and CuI complex on the surface of magnetic Fe_3O_4 nanoparticles. As can be seen, Fe–O stretching vibrations appeared near 579 cm^{-1} and O–H stretching vibrations appeared at 3400 cm^{-1}. As can be seen in the spectrum of Fe_3O_4@ABA-Aniline-CuI nanocatalyst, the C=N bending vibration bands show a clear shift towards lower frequency (1642 → 1624 cm^{-1}) compared to the Fe_3O_4@ABA-Aniline spectrum, which indicates complex formation between CuI with C–N ligands.[57]

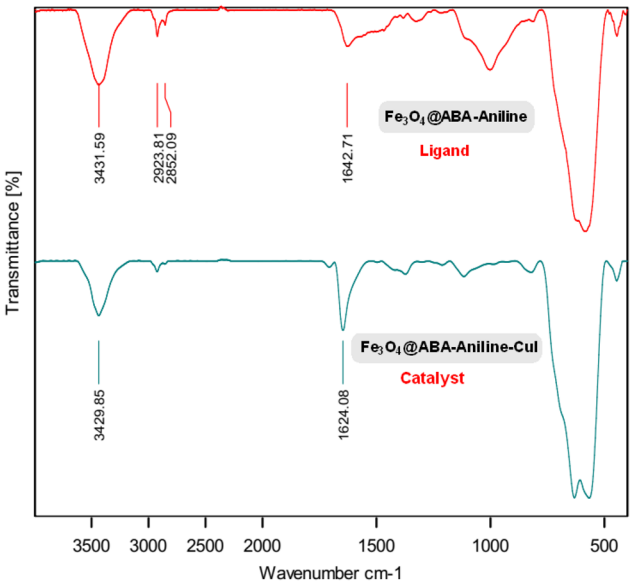

Fig. 2 FT-IR spectra of Fe_3O_4@ABA-Aniline ligand and Fe_3O_4@ABA-Aniline-CuI nanocatalyst.

Scanning electron microscopy (SEM)

Scanning electron microscopy (SEM) shows images of the surface of Fe_3O_4@ABA-Aniline-CuI catalyst with high magnification (Fig. 3). In this analysis, the surface of the catalyst is shown at high magnification and the SEM image confirms the sphericity of Fe_3O_4@ABA-Aniline-CuI nanoparticles.

Transmission electron microscopy (TEM)

Transmission electron microscopy (TEM) was used to accurately determine the shape and size of Fe_3O_4@ABA-Aniline-CuI particles. As shown in Fig. 4, the shape of the Fe_3O_4@ABA-Aniline-CuI particles is spherical and the size of the particles is approximately between 12–25 nanometers (nm).

X-ray diffraction analysis (XRD)

X-ray diffraction analysis (XRD) was used to determine the crystal structure and purity of the Fe_3O_4@ABA-Aniline-CuI nanocatalyst (Fig. 5). The peaks that appeared are attributed to the (220), (311), (400), (422), (511) and (440) planes, which indicate that the structure of the iron nanoparticle (Fe_3O_4) is maintained during functionalization.[58]

Energy dispersive X-ray (EDX)

Energy dispersive X-ray spectroscopy (EDX) was applied in order to identify the successful formation of Fe_3O_4@ABA-Aniline-CuI

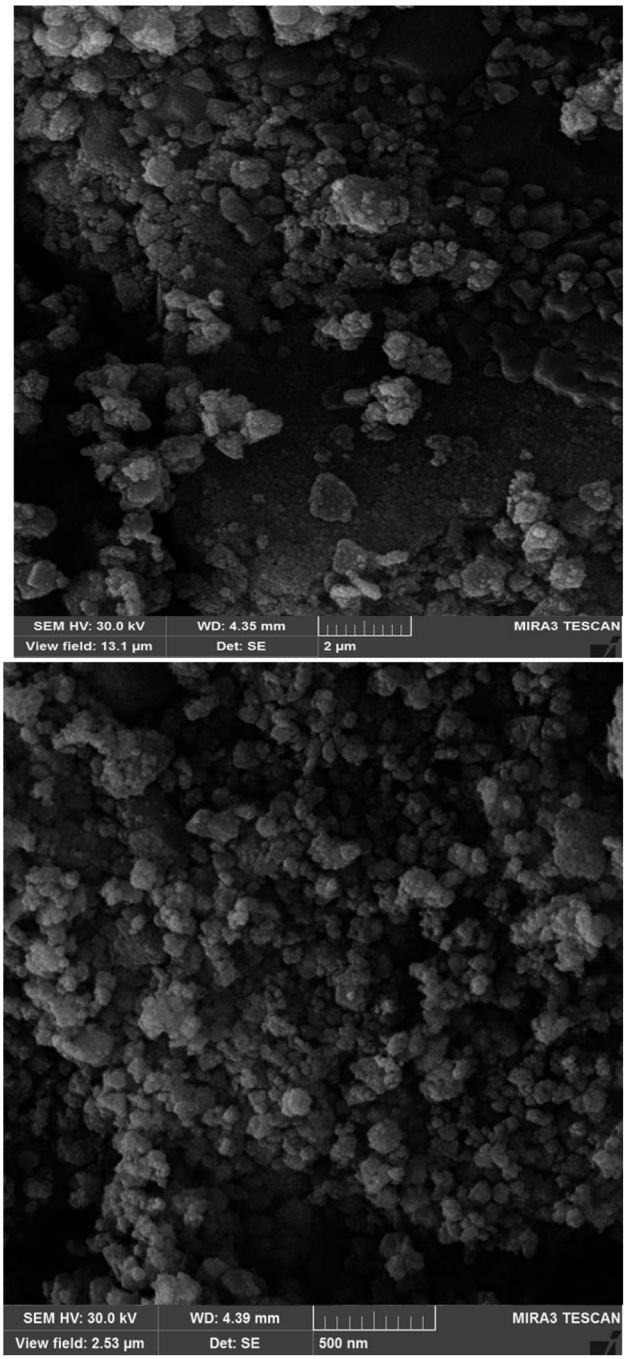

Fig. 3 SEM images of Fe_3O_4@ABA-Aniline-CuI nanocatalyst at different magnifications.

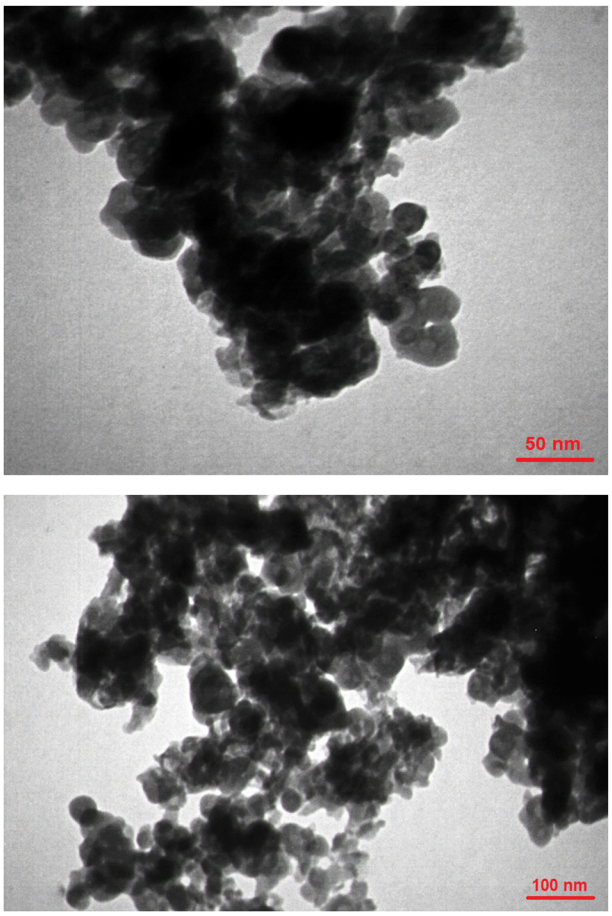

Fig. 4 TEM images of Fe_3O_4@ABA-Aniline-CuI nanocatalyst at different magnifications.

nanocatalyst. As shown in Fig. 6, the presence of the O peak confirms that the magnetic iron nanoparticle is surrounded by 4-aminobenzoic acid. Also, in this spectrum, the peaks of Fe, N and Cu elements can be seen, which is a confirmation of the successful synthesis of the catalyst.

Vibrating sample magnetometer (VSM)

The magnetic property of the synthesized nanocatalyst (Fe_3O_4@ABA-Aniline-CuI) was determined and investigated using a vibrating-sample magnetometer (VSM). As seen in Fig. 7, the magnetic property of the magnetic iron nanoparticle is 73.18 emu g^{-1}. By functionalizing the surface of the nanoparticle with Fe_3O_4@ABA-Aniline-CuI, this property was decreased to 36.07 emu g^{-1}, which indicates the stabilization of organic groups on the surface of the nanocatalyst.

Thermogravimetric analysis (TGA)

Thermogravimetric analysis (TGA) was used to determine the percentage of organic functional groups stabilized on the surface of the magnetic nanoparticles (Fig. 8). The organic groups adsorbed on the nanoparticle surface were decomposed at a high temperature of 260 °C. The weight loss of 17% at temperatures between 250–700 °C is related to the decomposition of organic groups stabilized on the magnetic iron nanoparticles. In total, TGA analysis showed that the catalyst has a weight loss of about 22.9%.

Inductively coupled plasma optical emission spectroscopy (ICP-OES)

ICP-OES analysis was used to determine the amount of Cu immobilized on the surface of the magnetic nanoparticles and it was determined that the amount of copper is 13.28 × 10^{-5} mmol g^{-1}.

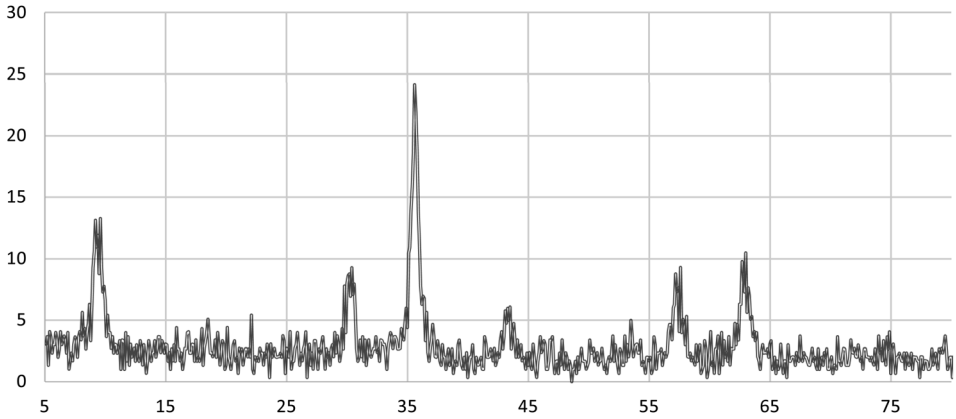

Fig. 5 XRD analysis of Fe_3O_4@ABA-Aniline-CuI nanocatalyst.

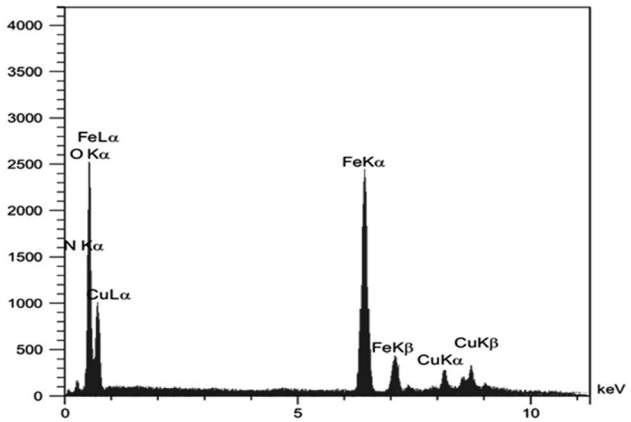

Fig. 6 EDX analysis of Fe_3O_4@ABA-Aniline-CuI nanocatalyst.

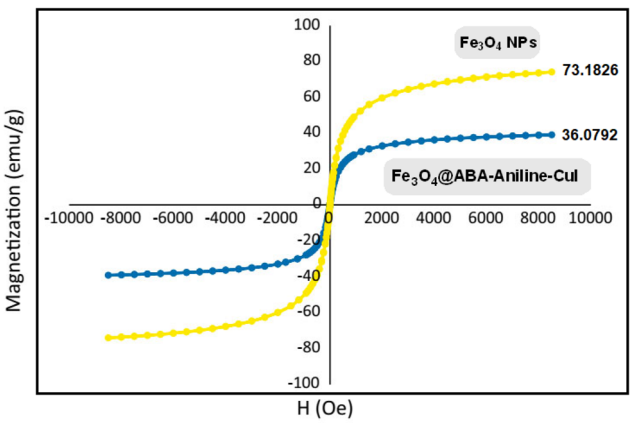

Fig. 7 VSM analysis of Fe_3O_4 NPs and Fe_3O_4@ABA-Aniline-CuI nanocatalyst.

Catalytic study

At the beginning of the laboratory work, the reaction of 2-iodoaniline (1, 0.5 mmol) with carbon disulfide (2, 1 mmol) and iodobenzene (3, 0.5 mmol) was selected as the model reaction and the optimization parameters for this reaction were investigated. First, the effect of the catalyst was evaluated on the preparation of model product **4a** (Table 1): no product was observed in the absence of catalyst. To investigate the effect of the catalyst, the model reaction was investigated in the presence of different catalysts [Fe_3O_4 NPs (5 mg), Fe_3O_4@ABA (5 mg), Fe_3O_4@ABA-BA (5 mg), Fe_3O_4@ABA-Aniline (5 mg) and Fe_3O_4@ABA-Aniline-CuI (5 mg)]. The maximum yield was seen when the model reaction was catalyzed by Fe_3O_4@ABA-Aniline-CuI nanocatalyst. Then, the effect of the catalyst amount on the progress of the reaction was investigated and it was found that amounts greater than 20 mg of Fe_3O_4@ABA-Aniline-CuI catalyst do not have much effect on the progress of the reaction. In this reaction, the nature of the solvent plays a vital role in the activity of the catalyst and the yield of the products. It is evident from the results obtained in Table 2 that the best result is obtained in polyethylene glycol 400 (PEG-400) as solvent at 100 °C. The product **4a** was obtained in good yields when the model reaction was carried out in dimethyl sulfoxide, dimethyl formamide and ethanol solvents. Also, the results showed that water solvent is not favorable for this reaction. Only 36% and 6% of product **4a** were obtained in toluene and solvent-free conditions, respectively.

Next, the role of the base in the model reaction was investigated and the reaction was carried out in the presence of different bases (Table 3). A category of bases was used for the

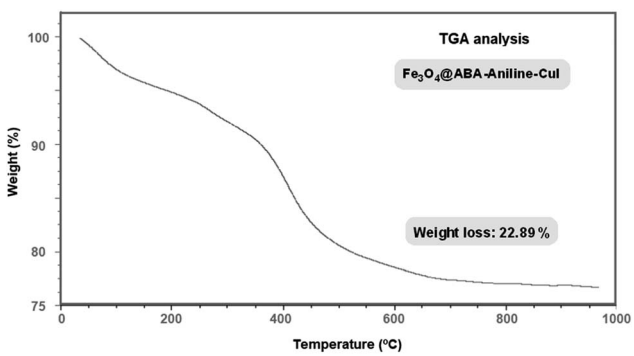

Fig. 8 TGA analysis of Fe_3O_4@ABA-Aniline-CuI nanocatalyst.

Table 1 Catalyst effect on the preparation of model product **4a**

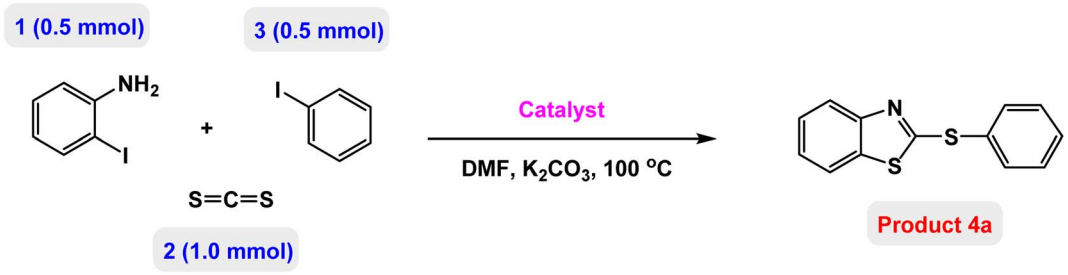

Entry	Catalyst (mg)	Time (h)	Yield[a] (%)
1	No catalyst	24	No
2	Fe_3O_4 NPs (5 mg)	6	4
3	Fe_3O_4@ABA (5 mg)	6	9
4	Fe_3O_4@ABA-BA (5 mg)	6	5
5	Fe_3O_4@ABA-Aniline (5 mg)	6	10
6	CuI (5 mg)	6	37
7	Fe_3O_4@ABA-Aniline-CuI (5 mg)	6	62
8	Fe_3O_4@ABA-Aniline-CuI (10 mg)	6	75
9	Fe_3O_4@ABA-Aniline-CuI (15 mg)	6	81
10	**Fe_3O_4@ABA-Aniline-CuI (20 mg)**	**6**	**86**
11	Fe_3O_4@ABA-Aniline-CuI (25 mg)	6	86

[a] Isolated yields.

synthesis of product **4a**; the reaction in the presence of two bases, potassium carbonate (K_2CO_3) and potassium acetate (KOAc) bicarbonate, gave the best results and KOAc was chosen as the optimal base. Then, to expand the scope of application of this catalytic system, a number of aryl and heteroaryl iodides were used for the synthesis of benzothiazole-sulfide aryl derivatives and the results of these experiments are summarized in Table 4. As shown in Table 4, iodobenzene derivatives carrying

Table 2 Solvent effect on the preparation of model product **4a**

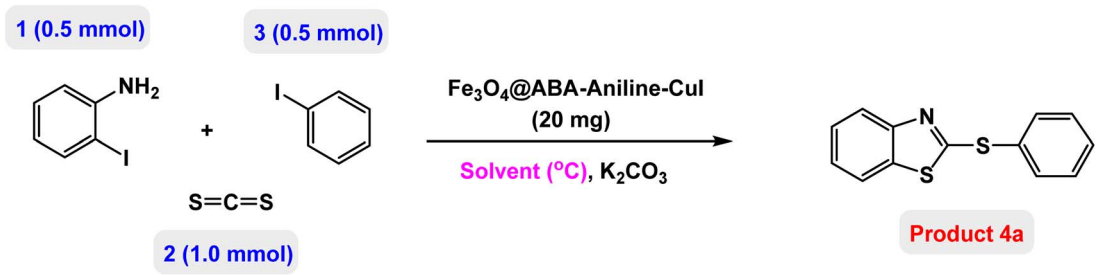

Entry	Solvent (°C)	Time (h)	Yield[a] (%)
1	DMF (100 °C)	6	86
2	EtOH (reflux)	6	83
3	H_2O (reflux)	6	52
4	DMSO (100 °C)	6	89
5	Toluene (100 °C)	6	36
6	**PEG-400 (100 °C)**	**6**	**91**
7	PEG-400 (110 °C)	6	91
8	PEG-400 (120 °C)	6	89
9	PEG-400 (90 °C)	6	87
10	Solvent-free (100 °C)	24	6

[a] Isolated yields.

Table 3 Base effect on the preparation of model product **4a**

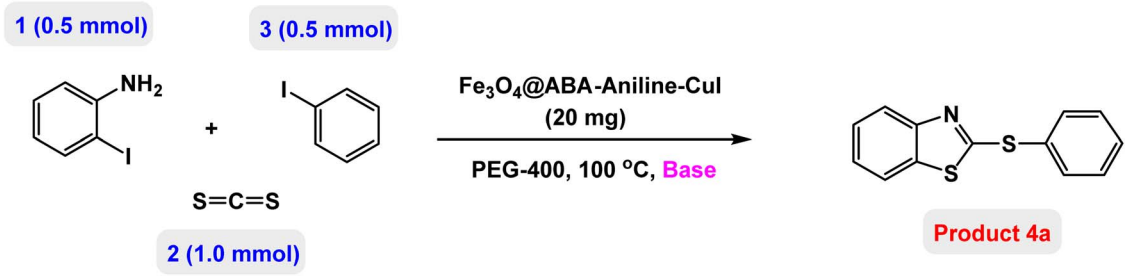

Entry	Base	Time (h)	Yield[a] (%)
1	K_2CO_3	6	91
2	Pyridine	6	72
3	DABCO	6	61
4	Et_3N	6	82
5	Cs_2CO_3	6	90
6	NaOH	6	55
7	*t*-BuOK	6	13
8	DBU	6	80
9	KOAc	**6**	94
10	No base	24	No

[a] Isolated yields.

electron-withdrawing and electron-donating groups obtain products in high to excellent yields. Also, various derivatives of heteroaryl iodides were used in the reaction with carbon disulfide and 2-iodoaniline and the benzothiazole-sulfide heteroaryl products were synthesized with high yields. Moreover, aryl bromides were found to be more easily reactive than aryl chlorides due to the latter being less reactive as electrophilic partners. This is because the reactivity of electrophilic partners is based on their leaving groups, with iodine being the most reactive followed by bromine, chlorine, and fluorine. Chloride electrophiles are the least reactive as they are less willing to participate in reactions.

Based on previous reports on the synthesis of benzothiazoles and diaryl sulfides in the presence of copper catalysts, we propose the following scheme for the synthesis of benzothiazole-sulfide aryls (product **4a** as model reaction) catalyzed by Fe_3O_4@ABA-Aniline-CuI nanocomposite (Scheme 2).

Reusability of Fe_3O_4@ABA-Aniline-CuI nanocatalyst

The possibility of recycling and reusing a catalyst in catalytic reactions is a very valuable factor. To achieve this goal, the reusability of Fe_3O_4@ABA-Aniline-CuI nanocatalyst was evaluated for the synthesis of product **4d** (as a model reaction) under the standardized conditions. After completion of the reaction, the catalyst was isolated by applying an external magnetic field. Then, the recovered catalyst was washed with ethyl acetate three times and used for the next reaction. The results clearly showed that the Fe_3O_4@ABA-Aniline-CuI catalyst can be reused at least 7 times without significant reduction in its catalytic activity (Fig. 9). ICP-OES analysis was used to determine the amount of Cu in the structure of the catalyst after 7 runs and results confirmed that the amount of copper is 13.22×10^{-5} mmol g^{-1}. Also, SEM and TEM techniques were used to study the structure and shape of the recovered nanocatalyst after 7 runs. As shown in Fig. 10 and 11, the shape of the nanoparticles is spherical and a little clumping and accumulation is observed in the nanoparticle structure.

Hot filtration and metal leaching tests

The nature of Fe_3O_4@ABA-Aniline-CuI composite catalyst was tested by hot filtration and ICP-OES metal leaching tests. The results showed that when the solid catalyst was removed, the conversion rate was only 1%, similar to the reaction without a catalyst. However, the ICP-OES analysis revealed that there was minimal Cu leaching into the reaction medium, indicating that the active components of the catalyst remained intact during the reaction.

Conclusion

In this paper, CuI was successfully immobilized on the surface of magnetic Fe_3O_4 nanoparticles modified with aniline and 4-aminobenzoic acid and its catalytic activity was investigated in the preparation of a broad range of benzothiazole-sulfide aryls and heteroaryls through the one-pot three-component reactions of 2-iodoaniline with carbon disulfide and aryl or heteroaryl iodides in the presence of KOAc as base in PEG-400 as solvent. The preparation of the catalyst from cheap and available raw materials, the efficiency of the catalyst in performing the reaction and its easy separation by applying an external magnetic field are the most important advantages of this catalytic system. The recycling results clearly showed that the Fe_3O_4@ABA-

Table 4 Scope of Fe_3O_4@ABA-Aniline-CuI nanocatalyst in synthesis of benzothiazole-sulfide aryls[a,b,c]

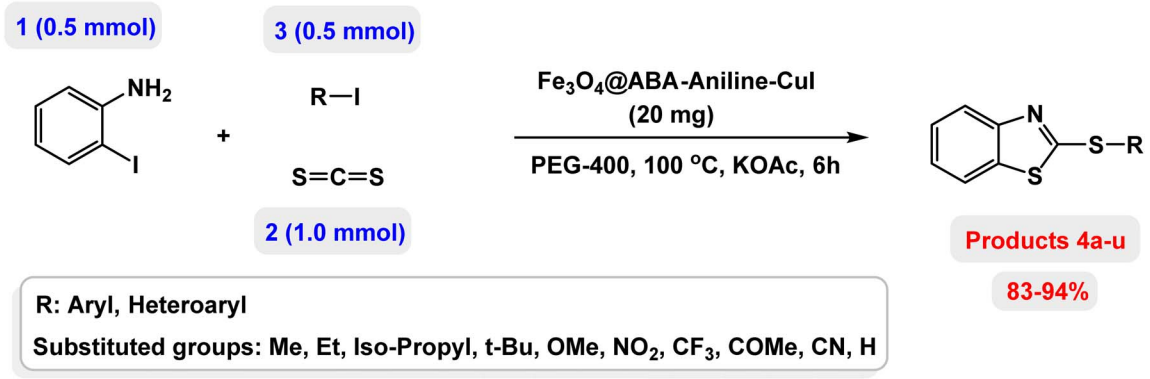

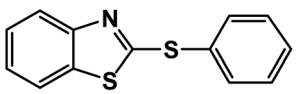
Product 4a
94%

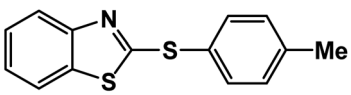
Product 4b
97%

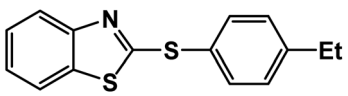
Product 4c
95%

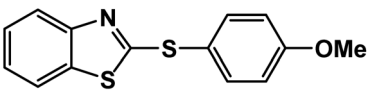
Product 4d
97%

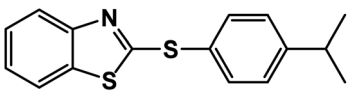
Product 4e
88%

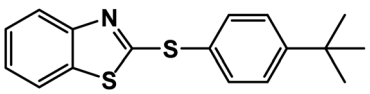
Product 4f
83%

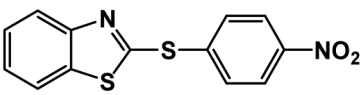
Product 4g
90%

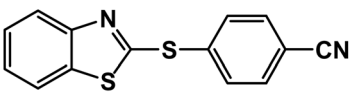
Product 4h
91%

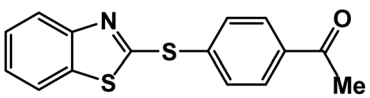
Product 4i
90%

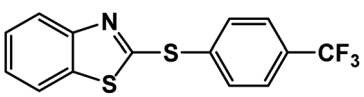
Product 4j
86%

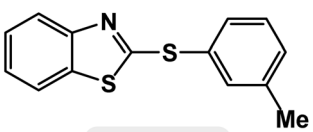
Product 4k
95%

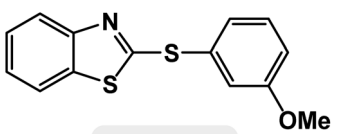
Product 4l
93%

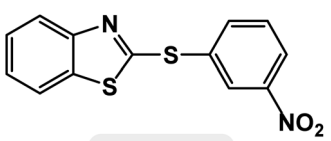
Product 4m
86%

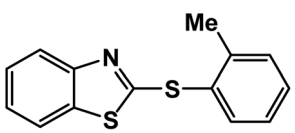
Product 4n
96%

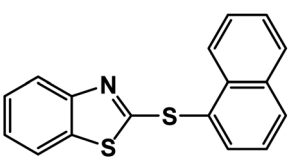
Product 4o
91%

Table 4 (*Contd.*)

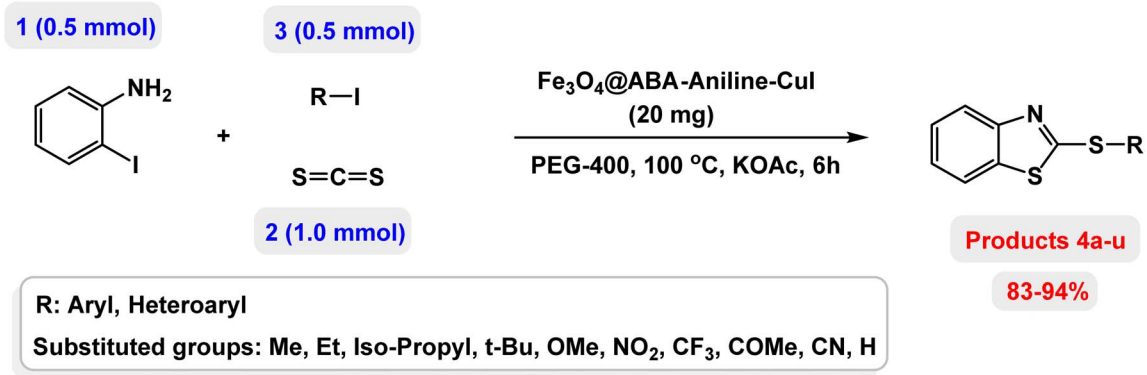

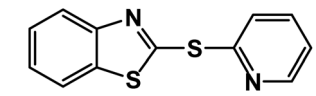
Product 4p
93%

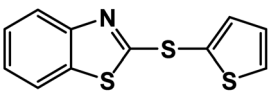
Product 4q
91%

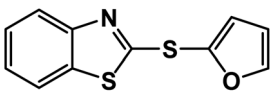
Product 4r
89%

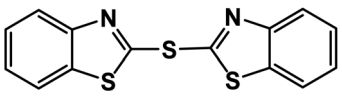
Product 4s
90%

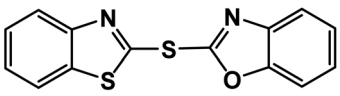
Product 4t
87%

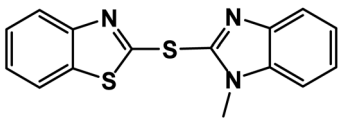
Product 4u
91%

b

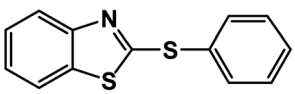
Product 4a
88%

c

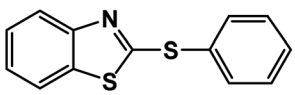
Product 4a
83%

[a] Isolated yields. [b] The reaction was carried out using bromobenzene. [c] The reaction was carried out using chlorobenzene.

Aniline-CuI catalyst can be reused at least 7 times without significant reduction in its catalytic activity.

Experimental

Materials and methods

The chemicals and solvents used were purchased from Merck and Sigma-Aldrich. The purity of the products and the progress of the reactions were checked by TLC on silica gel plates (SILG/UV254). FTIR (USA, PerkinElmer, 400–4000 cm^{-1}) was used to identify the catalyst functional groups. XRD patterns were examined at 2 theta = 20–80° (1.5405 Å = XRD-BRUKER) to define the nanoparticle crystallography. A STA503 instrument (Germany, BAHR, 30 °C to 800 °C, 10 °C min^{-1} rising rate, 70 cm^3 min^{-1} argon flow) was used for thermogravimetric analysis. EDX analysis (VEGA II Detector, TESCAN, Czech Republic) determined the elemental components on the heterogeneous catalyst surface. FESEM (FESEM/TE/SCAN, Philips) and TEM (TEM/CM 120, Philips) analyses examined the catalyst surface morphology. A vibrating sample magnetometer (VSM, model EZ-9, G. Colombo 81, 20133 Milano, Italy) measured the nanocatalyst's magnetic characteristics.

Preparation of Fe_3O_4@ABA-Aniline-CuI nanocomposite

First, Fe_3O_4 magnetic particles were synthesized through co-precipitation of Fe^{2+}/Fe^{3+} salt solution in an alkaline environment as previously reported.[59] The nanoparticles of Fe_3O_4 (1.0 g) were ultrasonically dispersed in a solution containing ethanol (100 ml) by ultrasonic irradiation for 30 minutes. Then, an

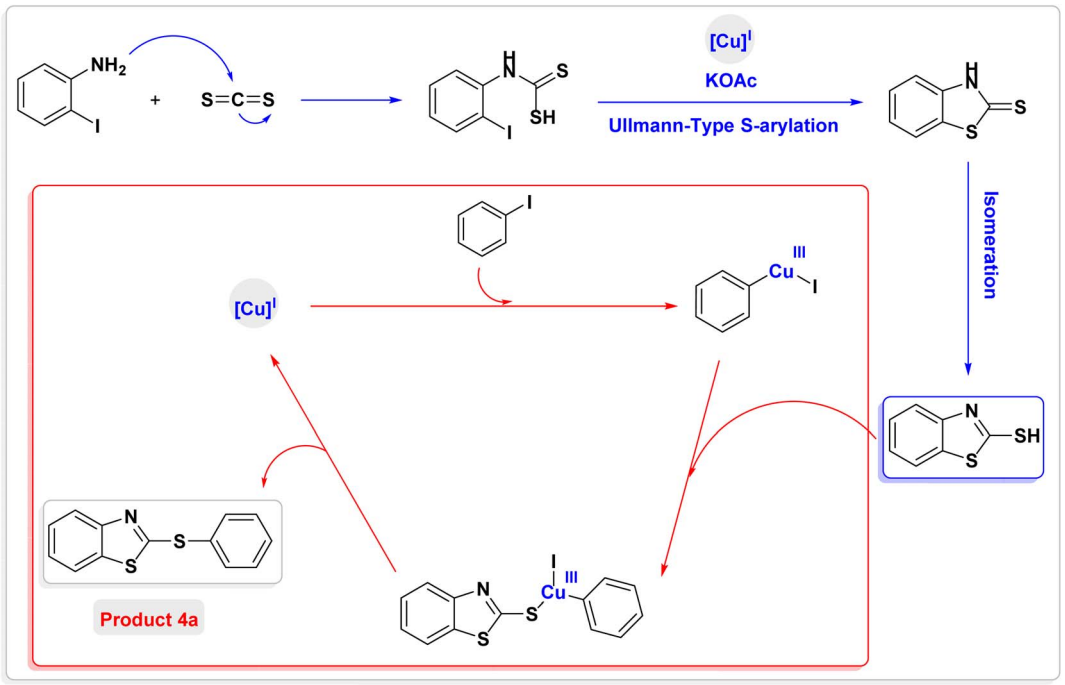

Scheme 2 Plausible mechanism for preparation of benzothiazole-sulfide aryls (product **4a** as model reaction) catalyzed by Fe_3O_4@ABA-Aniline-CuI nanocomposite.

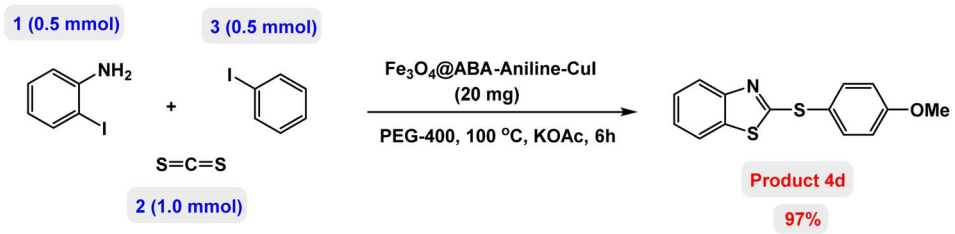

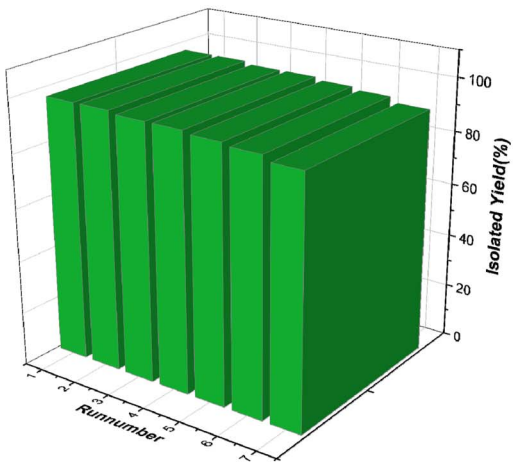

Fig. 9 Reusability of Fe_3O_4@ABA-Aniline-CuI nanocatalyst in preparation of product **4d**.

ethanolic solution of 4-aminobenzoic acid (3 mmol in 10 ml of ethanol) was added dropwise to the resulting suspension. After stirring for 2 h at reflux temperature, the Fe_3O_4@ABA particles were magnetically separated from the suspension and washed with DI water and ethanol. The desired magnetic nanoparticles were dried in the vacuum oven at 50 °C for 4 h. Aniline was introduced to the Fe_3O_4@ABA MNPs using a two-step procedure. The magnetic Fe_3O_4@ABA (1.0 g) was dispersed in 100 ml of

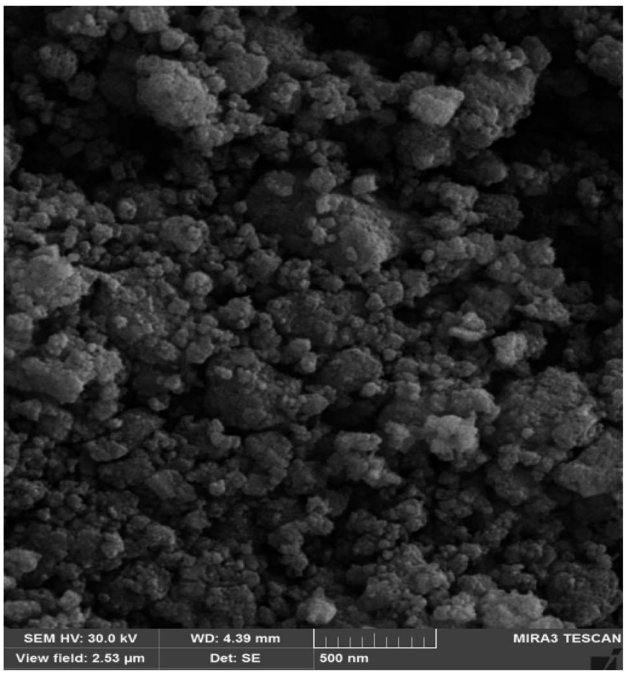

Fig. 10 SEM image of the recovered Fe_3O_4@ABA-Aniline-CuI nanocatalyst after 7 runs.

ethanol by ultrasonic irradiation for 30 min. Then, biacetyl (3 mmol) was added to the reaction medium. After stirring for 10 h at reflux temperature, the as-prepared magnetic Fe_3O_4@ABA-BA powder was magnetically separated from the suspension, rinsed with ethanol and dried in the vacuum oven at 50 °C for 4 h. In the next step, 1.0 g of dried magnetic Fe_3O_4@ABA-BA dispersed in 100 ml ethanol (ultrasonication for 30 min) was treated with 3 mmol aniline. After stirring for 10 h at reflux conditions in an inert gas atmosphere, the Fe_3O_4@ABA-Aniline nanocomposite particles were separated by magnetic decantation and the obtained powder was rinsed twice with ethanol to remove excess aniline. The final particles were dried in an oven at 60 °C for 4 h.

To synthesize Fe_3O_4@ABA-Aniline-CuI nanocatalyst, Fe_3O_4@ABA-Aniline (1.0 g) powder was sonicated for 30 min in 100 ml of DMF. Then, 3 mmol of CuI salt was added and the suspension was refluxed for 4 h in an inert gas atmosphere at 80 °C. The prepared particles were magnetically separated from the mixture and washed with ethanol three times. A vacuum oven was used to dry the final nanoparticles at 40 °C (Scheme 1).

General procedure for preparation of benzothiazole-sulfide aryls catalyzed by Fe_3O_4@ABA-Aniline-CuI nanocomposite

In a round bottomed flask, a mixture of 2-iodoaniline (0.5 mmol), carbon disulfide (1 mmol), KOAc (1.5 equiv) and Fe_3O_4@ABA-Aniline-CuI catalyst (20 mg) was stirred in PEG-400 at 100 °C for 2 h. Then, the aryl and heteroaryl iodides (0.5 mmol) were added to the reaction mixture and the reaction proceeded for 4 h, monitored by thin-layer chromatography (TLC). The Fe_3O_4@ABA-Aniline-CuI catalyst was easily separated with an external magnet, the organic layer was separated, and the aqueous layer was extracted with ethyl acetate. The obtained organic phase was dried over Na_2SO_4 and concentrated *in vacuo*. The crude material was purified with a chromatography column on silica gel (gradient eluent of EtOAc/petroleum ether) to give the benzothiazole-disulfide aryl and heteroaryl products.

NMR data for several examples of benzothiazole-sulfide aryls and heteroaryls

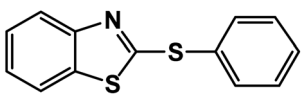

Product 4a

94%

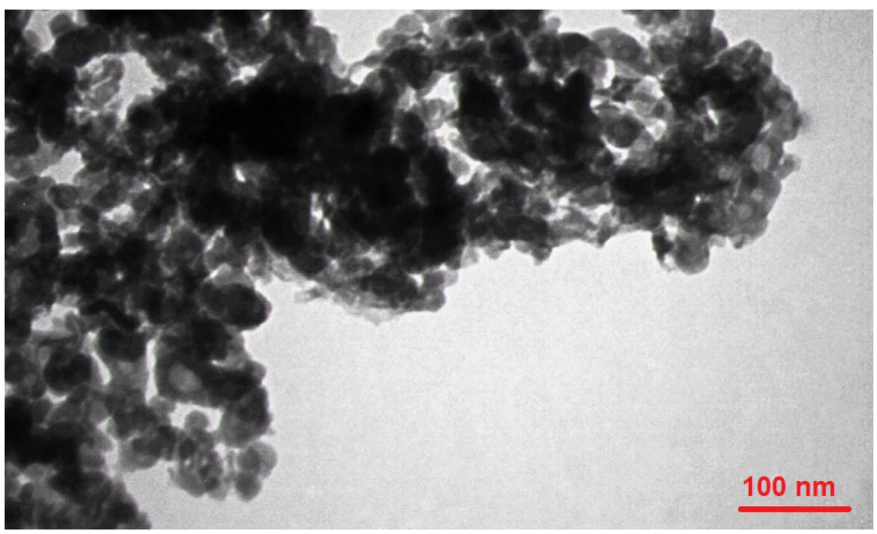

Fig. 11 TEM image of the recovered Fe_3O_4@ABA-Aniline-CuI nanocatalyst after 7 runs.

2-(Phenylthio)benzo[*d*]thiazole. ^{1}H NMR (500 MHz, $CDCl_3$) δ 8.04–8.01 (m, 2H), 7.62–7.60 (m, 2H), 7.59–7.45 (m, 5H); ^{13}C NMR (126 MHz, $CDCl_3$) δ 162.1, 135.9, 135.6, 134.8, 134.2, 130.5, 129.3, 129.2, 128.3, 127.2, 127.0, 126.1, 125.7, 124.3, 123.4.

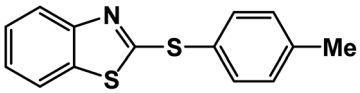

Product 4b

97%

2-(*p*-Tolylthio)benzo[*d*]thiazole. ^{1}H NMR (500 MHz, $CDCl_3$) δ 7.96 (dd, J = 7.8, 1.3 Hz, 1H), 7.54–7.51 (m, 2H), 7.51–7.47 (m, 3H), 7.46–7.42 (m, 2H), 7.40–7.26 (m, 1H), 2.49 (s, 3H); ^{13}C NMR (126 MHz, $CDCl_3$) δ 163.2, 138.4, 137.7, 135.9, 132.9, 132.7, 129.5, 129.3, 127.6, 1272, 124.8, 21.8.

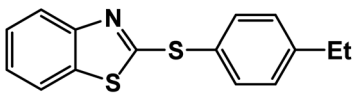

Product 4c

95%

2-((4-Ethylphenyl)thio)benzo[*d*]thiazole. ^{1}H NMR (400 MHz, $CDCl_3$) δ 8.08–8.02 (m, 2H), 7.62–7.56 (m, 1H), 7.56–7.42 (m, 2H), 7.42–7.30 (m, 2H), 7.28–7.24 (m, 1H), 2.30 (s, 2H), 1.3 (s, 3H); ^{13}C NMR (101 MHz, $CDCl_3$) δ 159.6, 143.6, 137.7, 136.4, 132.6, 130.8, 129.2, 128.7, 126.5, 125.8, 124.7, 26.5, 20.7.

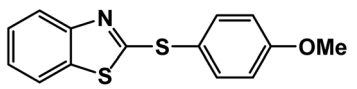

Product 4d

97%

2-((4-Methoxyphenyl)thio)benzo[*d*]thiazole. ^{1}H NMR (600 MHz, $CDCl_3$) δ 8.02 (d, J = 9.1 Hz, 2H), 7.60 (m, 2H), 7.45–7.43 (m, 2H), 6.97 (d, J = 9.0 Hz, 2H), 3.77 (s, 3H); ^{13}C NMR (126 MHz, $CDCl_3$) δ 158.6, 154.0, 136.1, 128.7, 128.4, 128.4, 128.2, 127.6, 113.8, 55.6.

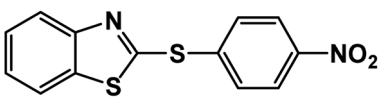

Product 4g

90%

2-((4-Nitrophenyl)thio)benzo[*d*]thiazole. ^{1}H NMR (500 MHz, $CDCl_3$) δ 8.07–8.02 (m, 2H), 7.51–7.50 (m, 2H), 7.50–7.43 (m, 2H), 7.19–7.15 (m, 2H); ^{13}C NMR (126 MHz, $CDCl_3$) δ 166.1, 164.0, 158.7, 136.1, 133.1, 133.1, 131.1, 131.0, 129.6, 129.3, 128.0, 117.0, 116.9.

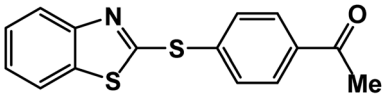

Product 4i

90%

1-(4-(Benzo[*d*]thiazol-2-ylthio)phenyl)ethan-1-one. ^{1}H NMR (500 MHz, $CDCl_3$) δ 8.11 (d, J = 8.0 Hz, 2H), 8.06 (d, J = 7.9 Hz, 2H), 7.52 (m, 2H), 7.50–7.46 (m, 2H), 2.67 (s, 3H); ^{13}C NMR (151 MHz, $CDCl_3$) δ 197.4, 163.7, 141.6, 139.9, 135.0, 130.8, 129.4, 128.6, 126.7, 125.7, 25.9.

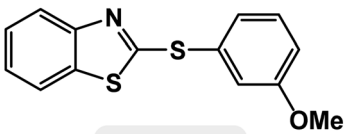

Product 4l

93%

2-((3-Methoxyphenyl)thio)benzo[*d*]thiazole. ^{1}H NMR (500 MHz, $CDCl_3$) δ 8.15 (d, J = 8.4 Hz, 2H), 8.06 (d, J = 8.6 Hz, 2H), 7.53–7.49 (m, 2H), 7.49–7.44 (m, 2H), 3.96 (s, 3H); ^{13}C NMR (126 MHz, $CDCl_3$) δ 165.1, 166.0, 138.9, 133.0, 133.4, 129.9, 128.7, 127.3, 126.4, 125.8, 52.8.

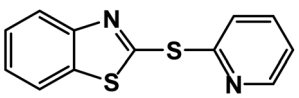

Product 4p

93%

2-(Pyridin-2-ylthio)benzo[*d*]thiazole. ^{1}H NMR (500 MHz, $CDCl_3$) δ 9.24 (d, J = 1.7 Hz, 1H), 8.82 (dd, J = 4.8, 1.6 Hz, 1H), 8.28 (ddd, J = 8.0, 2.2, 1.7 Hz, 1H), 7.57–7.45 (m, 4H), 7.44 (ddd, J = 8.0, 4.9, 0.8 Hz, 1H); ^{13}C NMR (126 MHz, $CDCl_3$) δ 161.8, 155.2, 149.7, 136.0, 135.8, 132.3, 129.9, 128.4, 126.3, 122.6.

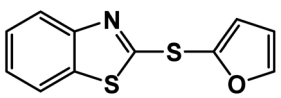

Product 4r

89%

2-(Furan-2-ylthio)benzo[*d*]thiazole. ^{1}H NMR (400 MHz, $CDCl_3$) δ 8.02 (d, J = 9.0 Hz, 2H), 7.43 (d, J = 8.9 Hz, 2H), 6.97 (d, J = 8.9 Hz, 2H), 6.91 (d, J = 9.0 Hz, 1H); ^{13}C NMR (101 MHz, $CDCl_3$) δ 164.6, 161.4, 137.5, 130.1, 129.4, 119.1, 115.4, 114.1.

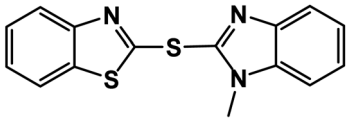

Product 4u

91%

2-((1-Methyl-1*H*-benzo[*d*]imidazole-2-yl)thio)benzo[*d*]thiazole. ^{1}H NMR (400 MHz, $CDCl_3$) δ 8.13 (d, J = 8.1 Hz, 1H), 7.87 (d, J = 8.3 Hz, 1H), 7.79 (dd, J = 8.2, 1.1 Hz, 1H), 7.60 (dd, J = 7.1, 1.2 Hz, 1H), 7.51–7.41 (m, 3H), 2.32 (s, 3H); ^{13}C NMR (101 MHz, $CDCl_3$) δ 163.8, 136.0, 134.2, 132.6, 128.7, 126.4, 125.1, 124.9, 123.1, 122.1, 31.0.

Conflicts of interest

There are no conflicts to declare.

References

1 M. J. Genzink, J. B. Kidd, W. B. Swords and T. P. Yoon, *Chem. Rev.*, 2022, **122**, 1654–1716.
2 A. D. Zahra Hoseini, *Adv. J. Chem. A*, 2021, **4**, 68–77.
3 J. Luo, Y. Liu, H. Wang, C. Gong, Z. Zhou and Q. Zhou, *Heterocycles*, 2022, **104**, 123.
4 Z. Zhang, Z.-W. Hou, H. Chen, P. Li and L. Wang, *Green Chem.*, 2023, **25**, 3543–3548.
5 X. Lei, Q. Tang, Y. Zheng, P. Kidkhunthod, X. Zhou, B. Ji and Y. Tang, *Nat. Sustain.*, 2023, 1–11.
6 A. Dehno Khalaji, M. Jarosova and P. Machek, *Asian J. Green Chem.*, 2021, **5**, 351–358.
7 M. B. Chaudhari and B. Gnanaprakasam, *Chem. – Asian J.*, 2019, **14**, 76–93.
8 S. Gupta, *J. Synth. Chem.*, 2022, **1**, 37–41.
9 R. Qiu, W. Wang, Z. Wang and H. Wang, *Catal. Sci. Technol.*, 2023, **13**, 2566–2584.
10 L. Kong, H. Sun, Y. Nie, Y. Yan, R. Wang, Q. Ding, S. Zhang, H. Yu and G. Luan, *Molecules*, 2023, **28**, 2681.
11 W. Guo, H. Luo, Z. Jiang, D. Fang, J. Chi, W. Shangguan, Z. Wang, L. Wang and A. F. Lee, *ACS Catal.*, 2022, **12**, 12000–12013.
12 H. Li, S. Zhao, W. Zhang, H. Du, X. Yang, Y. Peng, D. Han, B. Wang and Z. Li, *Fuel*, 2023, **342**, 127786.
13 J. Liu, X. Qu, C. Zhang, W. Dong, C. Fu, J. Wang and Q. Zhang, *J. Cleaner Prod.*, 2022, **377**, 134228.
14 B. Ji, J. Gou, Y. Zheng, X. Pu, Y. Wang, P. Kidkhunthod and Y. Tang, *Adv. Mater.*, 2023, 2300381.
15 F. Dhaouadi, L. Sellaoui, S. Taamalli, F. Louis, A. El Bakali, T. R. S. Cadaval Junior, A. Bonilla-Petriciolet, J. L. Marques Junior, A. VallerãoIgansi, T. S. Frantz, S. Frantz lütke, G. L. Dotto, L. A. De Almeida Pinto and A. Ben Lamine, *J. Mol. Liq.*, 2021, **343**, 117617.
16 H. Yu, J. Zhu, R. Qiao, N. Zhao, M. Zhao and L. Kong, *ChemistrySelect*, 2022, **7**(2), e202103668.
17 Z. Wan, T. Zhang, Y. Liu, P. Liu, J. Zhang, L. Fang and D. Sun, *Environ. Res.*, 2022, **213**, 113637.
18 D. Chen and T. Savidge, *Science*, 2015, **349**, 936.
19 P. Dong, Y. Zhang, S. Zhu, Z. Nie, H. Ma, Q. Liu and J. Li, *Metals*, 2022, **12**, 1160.
20 J. Singh, S. Juneja, R. K. Soni and J. Bhattacharya, *J. Colloid Interface Sci.*, 2021, **590**, 60–71.
21 L. Kong, Y. Liu, L. Dong, L. Zhang, L. Qiao, W. Wang and H. You, *Dalton Trans.*, 2020, **49**, 1947–1954.
22 M. Ghobadi, *J. Synth. Chem.*, 2022, **1**, 84–96.
23 B. Baghernejad and A. Zakariayi, *Asian J. Nanosci. Mater.*, 2022, **5**, 225–233.
24 G. Xia, Y. Zheng, Z. Sun, S. Xia, Z. Ni and J. Yao, *Environ. Sci. Pollut. Res.*, 2022, **29**, 39441–39450.
25 Z. Wang, C. Chen, H. Liu, D. Hrynshpan, T. Savitskaya, J. Chen and J. Chen, *Sci. Total Environ.*, 2020, **708**, 135063.
26 B. B. L. Nazari, *Eurasian Chem. Commun.*, 2021, **3**, 319–326.
27 P. Xu, Q. Yuan, W. Ji, R. Yu, F. Wang and N. Huo, *Mater. Express*, 2022, **12**, 1493–1501.
28 M. Ghobadi, M. Kargar Razi, R. Javahershenas and M. Kazemi, *Synth. Commun.*, 2021, **51**, 647–669.
29 Y. Liu, B. Fan, B. Xu and B. Yang, *Mater. Lett.*, 2023, **337**, 133979.
30 L. Wang, B. Ji, Y. Zheng and Y. Tang, *Angew. Chem., Int. Ed.*, 2023, **62**(18), e202301711.
31 M. Kazemi and M. Ghobadi, *Nanotechnol. Rev.*, 2017, **6**, 549–571.
32 H. Chen, C. Xu, F. Zhao, C. Geng, Y. Liu, J. Zhang, Q. Kang and Z. Li, *Appl. Surf. Sci.*, 2023, **609**, 155447.
33 Z. Wang, L. Dai, J. Yao, T. Guo, D. Hrynsphan, S. Tatsiana and J. Chen, *Chemosphere*, 2021, **281**, 130718.
34 R. Hudson, Y. Feng, R. S. Varma and A. Moores, *Green Chem.*, 2014, **16**, 4493–4505.
35 M. Lakshman, *J. Synth. Chem.*, 2022, **1**, 48–51.
36 V. K. Booramurthy, R. Kasimani, S. Pandian and D. Subramanian, *Arab. J. Sci. Eng.*, 2022, **47**, 6341–6353.
37 W. Huang, Q. Cheng and D. Ma, *Synth. Commun.*, 2021, **51**, 1321–1339.
38 N. Moeini, M. Ghadermazi and S. Molaei, *J. Mol. Struct.*, 2022, **1251**, 131982.
39 N. Alishahi, M. Nasr-Esfahani, I. Mohammadpoor-Baltork, S. Tangestaninejad, V. Mirkhani and M. Moghadam, *Appl. Organomet. Chem.*, 2020, **34**(8), e5681.
40 D. Chen, Q. Wang, Y. Li, Y. Li, H. Zhou and Y. Fan, *Chemosphere*, 2020, **247**, 125869.
41 X. Zhang, M. Aqeel Ashraf, Z. Liu and D. Zhang, *Synth. Commun.*, 2020, **50**, 2705–2734.
42 J. Le Bescont, C. Breton-Patient and S. Piguel, *Eur. J. Org. Chem.*, 2020, **2020**, 2101–2109.
43 X. Gao, J. Liu, X. Zuo, X. Feng and Y. Gao, *Molecules*, 2020, **25**, 1675.
44 Z. Liu, B. Fan, J. Zhao, B. Yang and X. Zheng, *Corros. Sci.*, 2023, **212**, 110957.
45 Y. I. Asiri, A. Alsayari, A. B. Muhsinah, Y. N. Mabkhot and M. Z. Hassan, *J. Pharm. Pharmacol.*, 2020, **72**, 1459–1480.
46 H. T. Nguyen, T. H. Nguyen, D. D. Pham, C. T. Nguyen and P. H. Tran, *Heliyon*, 2021, **7**, e08309.

47 S. Dhadda, A. K. Raigar, K. Saini, Manju and A. Guleria, *Sustainable Chem. Pharm.*, 2021, **24**(1), 100521.
48 R. Isshiki, M. B. Kurosawa, K. Muto and J. Yamaguchi, *J. Am. Chem. Soc.*, 2021, **143**, 10333–10340.
49 T. Shibata, T. Iwaki and M. Ito, *Adv. Synth. Catal.*, 2022, **364**, 3472–3476.
50 S. Gupta, *J. Synth. Chem.*, 2022, **1**, 16–21.
51 P. Shinde and C. S. Rout, *Mater. Chem. Front.*, 2021, **5**, 516–556.
52 L. Chen, A. Noory Fajer, Z. Yessimbekov, M. Kazemi and M. Mohammadi, *J. Sulfur Chem.*, 2019, **40**(4), 451–468.
53 N. Sundaravelu, S. Sangeetha and G. Sekar, *Org. Biomol. Chem.*, 2021, **19**, 1459–1482.
54 Z. Gan, Q. Yan, G. Li, Q. Li, X. Dou, G. Li and D. Yang, *Adv. Synth. Catal.*, 2019, **361**, 4558–4567.
55 G. Kibriya, A. K. Bagdi and A. Hajra, *J. Org. Chem.*, 2018, **83**, 10619–10626.
56 K. Monir, A. K. Bagdi, M. Ghosh and A. Hajra, *J. Org. Chem.*, 2015, **80**, 1332–1337.
57 T. Cheng, D. Zhang, H. Li and G. Liu, *Green Chem.*, 2014, **16**, 3401–3427.
58 M. F. Kamel Ariffin and A. Idris, *Renewable Energy*, 2022, **185**, 1362–1375.
59 H. Khandaka and R. Kumar Joshi, *Tetrahedron Lett.*, 2022, **111**, 154163.